BUTTERWORTH HEINEMANN

Polymer Vol. 36 No. 11, pp. 2123–2131, 1995
Copyright © 1995 Elsevier Science Ltd
Printed in Great Britain. All rights reserved
0032-3861/95/$10.00 + 0.00

X-ray analysis and molecular modelling of the structure of aromatic copolyimides

Tzong-Ming Wu, Sergei Chvalun* and John Blackwell†
Department of Macromolecular Science, Case Western Reserve University, Cleveland, OH 44106-7202, USA

and Stephen Z. D. Cheng, Zongquan Wu and Frank W. Harris
Institute and Department of Polymer Science, College of Polymer Science and Polymer Engineering, University of Akron, Akron, OH 44325-3909, USA
(Received 26 May 1994; revised 12 October 1994)

X-ray diffraction and molecular mechanics modelling have been used to investigate the structures of two families of aromatic copolyimides. The first of these is synthesized by the reaction of 2,2′-bis(trifluoromethyl)-4,4′-diaminobiphenyl (PFMB) with a mixture of 3,3′,4,4′-biphenyltetracarboxylic dianhydride (BPDA) and pyromellitic dianhydride (PMDA); the second is synthesized from BPDA and a mixture of *o*-tolidine (OTOL) and *p*-phenylene diamine (PPD). The X-ray fibre diagram of 70/30 copoly(BPDA-PFMB/PMDA-PFMB) is very similar to that of homopoly(BPDA-PFMB), except that it is more diffuse. It appears that the structure is highly blocky, and the main effect of introduction of comonomer is to reduce the crystallinity of the poly(BPDA-PFMB) blocks. In contrast, the X-ray data for the copoly(BPDA-OTOL/BPDA-PPD) are non-periodic along the fibre direction, and the layer-line positions are reproduced by a model consisting of parallel arrays of extended chains of completely random sequence. Interestingly, the correlation length for the extended chain is larger in the copolymer than in homopolymer BPDA-OTOL, in contrast to those seen for the copoly(BPDA-PFMB/PMDA-PFMB) series. It is suggested that this is due to the fact that 'kink' distortions are less disruptive in copoly(BPDA-OTOL/BPDA-PPD).

(Keywords: aromatic copolyimides; X-ray diffraction; molecular mechanics modelling)

INTRODUCTION

In the present paper we describe investigations of the structure of aromatic copolyimides using X-ray diffraction methods, coupled with molecular mechanics modelling of their chain conformations. The copolyimides are synthesized by the condensation reaction between dianhydrides and diamines: the dianhydrides are 3,3′,4,4′-biphenyltetracarboxylic dianhydride (BPDA) and pyromellitic dianhydride (PMDA), and the diamines are 2,2′-bis(trifluoromethyl)-4,4′-diaminobiphenyl (PFMB), *o*-tolidine (OTOL) and *p*-phenylene diamine (PPD). Specifically we have studied the copolymers shown in *Figure 1*: these are copoly(BPDA-PFMB/PMDA-PFMB) and copoly(BPDA-OTOL/BPDA-PPD), which are further abbreviated to copoly(BFPF) and copoly(BTBD).

Aromatic polyimides are well known for their excellent thermal, mechanical and electrical properties, and their outstanding light stability[1,2]. However, the inherent chain rigidity leads to high glass transition and melting temperatures, with the result that polymers such as Kapton® and Vespel® are not melt processable[3] and must be processed from solution. However, the solubility of these polymers is also limited. Introduction of comonomers can improve the solubility, and the tensile properties are not diminished provided that the orientation of extended rod-like chains is retained. In this regard, analogies can be made to wholly aromatic polyesters, for which it is possible to reduce their melting temperatures and improve processability by the incorporation of comonomers that weaken the intermolecular interactions[4–6]. For the aromatic copolyimides, the use of heterocyclic comonomers often leads to physical and mechanical properties that exceed those of the component homopolymers[7,8]. In the case of copoly(BTBD), Cheng and co-workers[9] showed that introduction of BPDA-PPD leads to improvement in the mechanical properties, drawability and thermal stabilities compared to those for the homopoly(BPDA-OTOL).

At present, relatively little is known about the microstructure of BFPF and BTBD copolymers. These materials are synthesized from mixtures of the comonomers, either as a 'one-step' process or via various prepolymer routes. N.m.r. is not effective for analysis of sequence distribution because of the large size of the aromatic monomers and the alternating diamine–dianhydride structure. However, these systems are ideal for analysis by X-ray methods, by application of the methods that have been developed for analogous wholly aromatic copolyesters and copolyamides[10–14]. In the latter copolymers, the fibre diagrams contain non-periodic layer lines at positions that depend on the monomer ratios and sequence statistics. The

* Permanent address: Karpov Institute of Physical Chemistry, Moscow, Russia
† To whom correspondence should be addressed

Copoly(BFPF)

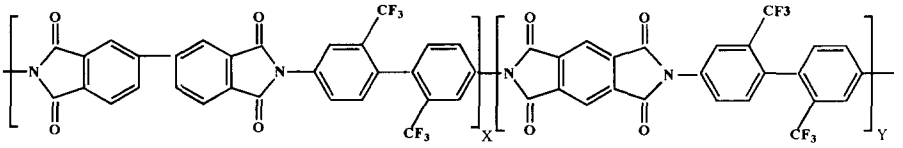

Copoly(BTBD)

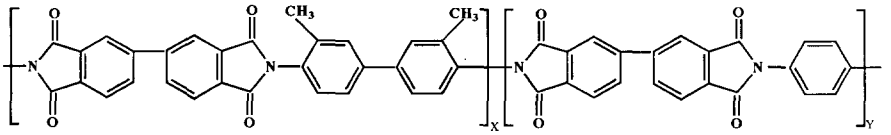

Figure 1 Chemical structures of copoly(BFPF) and copoly(BTBD)

advance per monomer along the chain is approximately constant for each monomer type, but these advances differ for the different monomers, depending on their chemical structures. Thus one proceeds along the chain in a statistical sequence of steps of two or more lengths. The diffraction characteristics are derived by evaluating the Fourier transform of the nearest-neighbour correlation function. Modification of the terms in the correlation function allows for consideration of both random and non-random comonomer sequences. For the copolyesters, the non-periodic layer lines are predicted by a structure consisting of extended chains of completely random sequences, and all but minimal non-randomness could be ruled out: these copolymers are thought to randomize via transesterification in the melt during synthesis. However, this may not be the case for the present copolyimides, which are synthesized in solution under conditions where the monomers may have very different reactivity ratios.

The two series of copolyimides to be considered here have extended, wholly aromatic structures, and their fibre diagrams can be treated in a similar manner to those for the copolyesters described above. We have utilized the X-ray data for some of the homopolymers, together with standard molecular mechanics modelling, in order to derive models for the monomers of the copolymer chains, and have analysed the X-ray data for both series of copolyimides in terms of their microstructures.

EXPERIMENTAL

Synthesis

Homopolymers. Homopoly(BPDA-PFMB) was synthesized from 3,3′,4,4′-biphenyltetracarboxylic dianhydride (BPDA) and 2,2′-bis(trifluoromethyl)-4,4′-diaminobiphenyl (PFMB) diamine. Detailed synthesis routes have been described previously[15–17]. In brief, equimolar proportions of the dianhydride and diamine were dissolved in *m*-cresol containing 2% (w/v) isoquinoline as catalyst, with a total solids content of approximately 12% (w/w). The solution was then heated under reflux for 6 h at 200°C. The intermediate poly(amic acid) precursor was not isolated, and imidization occurred spontaneously in the solution. The water liberated by the polycondensation was removed by distillation. The homopoly(BPDA-PFMB) had an intrinsic viscosity of 5.0 dl g^{-1} in *m*-cresol at 60°C.

Homopoly(BPDA-OTOL) was synthesized in a similar manner from BPDA and *o*-tolidine (OTOL) in *p*-chlorophenyl solution at 210°C under reflux for 6 h[9]. The resultant polymer had an intrinsic viscosity of 9.3 dl g^{-1} in *p*-chlorophenyl at 60°C.

Copoly(BFPF). Since homopoly(PMDA-PFMB) is insoluble in *m*-cresol, the copolyimides were synthesized from macromonomer intermediates. Intermediate A was prepared by reacting 1 mol of BPDA with 2 mol of PFMB in *m*-cresol at 200°C, and probably consisted predominantly of PFMB-BPDA-PFMB. Intermediate B was prepared from 2.0 mol of PFMB and 1.4 mol of BPDA, and was probably mainly a mixture of PFMB-BPDA-PFMB and PFMB-(BPDA-PFMB)$_2$. Three specimens of 70/30 copoly(BFPF) were prepared as follows.

Preparation I. PMDA (0.6 mol) and 0.4 mol of BPDA were added to the solution of macromonomer intermediate A and allowed to react for 6 h at 200°C, after which the water was removed by distillation[18]. As will be seen below, this protocol resulted in a highly blocky copolymer, suggesting very different reactivities for BPDA and PMDA. Preparations II and III were used in efforts to prepare less blocky 70/30 copolymers[19].

Preparation II: PMDA (0.6 mol) was added to the solution of intermediate A and allowed to react for 6 h at 200°C. The remaining 0.4 mol of BPDA was then added and the temperature maintained for a further 6 h, after which the water was removed by distillation.

Preparation III. PMDA (0.6 mol) was added to the solution of intermediate B and maintained at 200°C for 6 h, followed by removal of water by distillation.

All three copoly(BFPF) preparations had intrinsic viscosities in the range of 2.5–3.0 dl g^{-1}.

Copoly(BTBD). Copolymers with three different compositions were prepared in *p*-chlorophenyl solution by mixing 1 mol of BPDA with a total of 1 mol of OTOL and PPD at OTOL/PPD molar ratios of 80/20, 70/30 and 60/40. The mixtures were then heated at 210°C under reflux for 6 h, and the water was removed by distillation.

In addition, a 50/50 BTBD poly(amid acid) was prepared from 1 mol of BPDA and 1 mol of OTOL and PPD at OTOL/PPD molar ratio of 50/50 in a 10% (w/v) solution in *N*-methylpyrrolidone at 200°C. The solvent was evaporated to form a film on glass, and the polymer was imidized by heating to 200°C for 2 h.

Orientation procedures

Oriented fibres were prepared by dry-jet wet spinning of the above isotropic solutions into a water/methanol coagulation bath. The as-spun fibres were drawn in air at different temperatures (in the range of 320–480°C) to obtain maximum draw ratios[9,15]. The draw ratios obtained were 10× for homopoly(BPDA-PFMB), 5× for 70/30 copoly(BFPF), 2× for homopoly(BPDA-OTOL), and 5×, 8× and 12× for 80/20, 70/30 and 60/40 copoly(BTBD), respectively.

The film specimen of 50/50 copoly(BTBD) was drawn 4× at 300–350°C.

X-ray diffraction

Specimens for X-ray diffraction were prepared as bundles of about 15–20 fibres. X-ray fibre diagrams were recorded on Kodak Direct Exposure X-ray film (DEF 5) using a Searle toroidal camera and CuKα radiation. The observed *d*-spacings were calibrated by dusting the sample with CaF_2 powder. Linear $\theta/2\theta$ X-ray intensity scans of the fibres along the meridional (fibre axis) direction were recorded using Phillips PN 3550/10 and Rigaku D/Max diffractometers in the transmission mode, with Ni-filtered CuKα radiation. The most accurate measurements of *d*-spacings are for the intense meridional maxima on the third layer line of homopoly(BPDA-PFMB) and copoly(BFPF) and fourth layer line of homopoly(BPDA-OTOL) and copoly(BTBD), and are from the diffractometer data.

The longitudinal crystallite sizes and paracrystalline distortion parameters *g* for homopoly(BPDA-PFMB) and 70/30 copoly(BFPF) were derived from the integral half-widths of several orders of reflections for BFPF, using the Hosemann equation[20]:

$$\delta^2 = 1/L_{hkl}^2 + (\pi g n)^4/d_{hkl}^2 \qquad (1)$$

where δ is the integral half-width of reflection; L_{hkl} is the mean dimension of the crystallite perpendicular to (*hkl*) plane; d_{hkl} is the interplane spacing; g is the parameter of paracrystallinity; and n is the order of the reflection. Silicon powder (325 mesh size) was used as a standard in order to evaluate the instrumental broadening. For copoly(BTBD), the data are non-periodic, and the line broadening arises from the random comonomer structure, as well as the physical ordering. Efforts to delineate these two effects will be described in a further paper[21]. For the present purposes, the apparent crystallite sizes in the fibre axis direction were derived from the integral half-widths of the meridional maxima using the Scherrer equation. These data give an indication of the correlation length for the extended conformation of the copolymer chains.

The degree of orientation for each copolyimide was determined from the X-ray patterns of single filaments recorded on film. The specimens were tilted to the Bragg angle for the third layer line meridional reflection of homopoly(BPDA-PFMB) and 70/30 copoly(BFPF), and for the fourth layer line for homopoly(BPDA-OTOL) and 80/20, 70/30, 60/40, 50/50 copoly(BTBD). The azimuthal half-widths of the meridional reflections were measured using an Optronics P-1000 digital microdensitometer. The aperture and stepping raster were 100 μm; the detector range was set at 2.0 optical density.

Predicted scattering for extended chains of random sequence for copoly(BTBD)

The X-ray scattering of extended copolymer chains was calculated following reference 12. Atomic coordinates for the monomer residues were based on the bond lengths, bond angles and torsion angles derived from the model compound of pyromellitic dianhydride-oxydianiline[22], and standard data sources. Molecular mechanics energy minimizations for the homopolymer chains were carried out using the SYBYL® software package (Tripos Inc.). It will be seen that the minimum energy conformations match the observed fibre repeats derived from the X-ray data for the homopolymers. The predictions of the scattering by random copolyimides along the fibre axis direction were based on models with axial advances of 20.24 Å for BPDA-PFMB, 16.79 Å for PMDA-PFMB, 20.44 Å for BPDA-OTOL and 16.09 Å for BPDA-PPD.

RESULTS AND DISCUSSION

Copoly(BFPF)

Figure 2 shows X-ray diffraction patterns for drawn fibres of the homopoly(BPDA-PFMB) and 70/30 copoly-

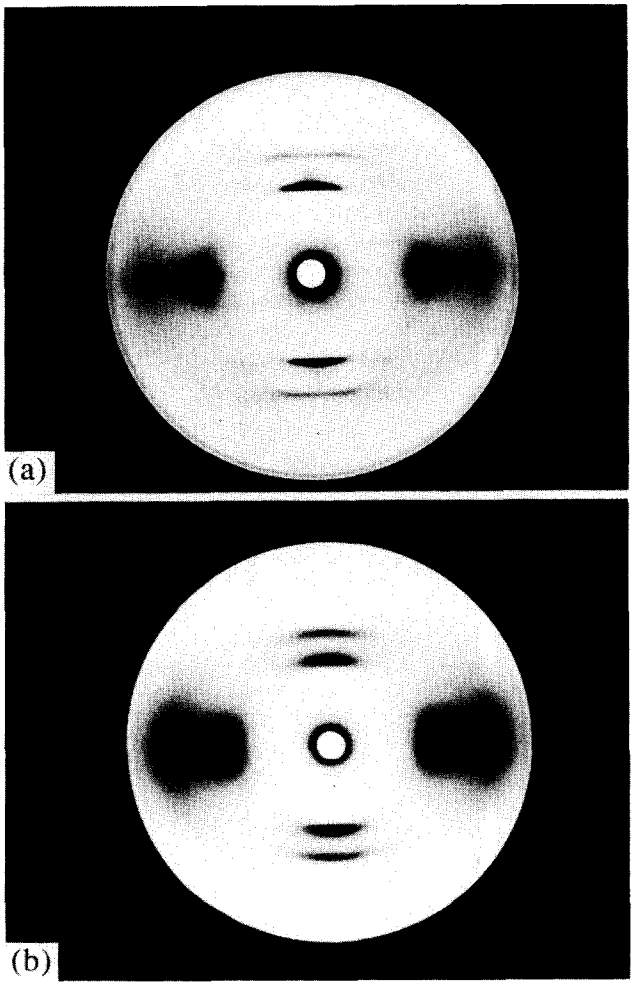

Figure 2 X-ray fibre diagrams of (a) homopoly(BPDA-PFMB) and (b) 70/30 copoly(BFPF)

(BFPF). For homopoly(BPDA-PFMB), the X-ray diffraction patterns reveal high orientation along the fibre axis. We observe numerous Bragg reflections on the equator and several layer lines. From measurement of the distinct layer line streaks, the observed repeat in the chain axis direction is $c = 20.24 \pm 0.02$ Å. *Table 1* compares the *d*-spacings of the observed layer lines and the calculated *d*-spacings based on the observed fibre repeat.

The chemical structure of the BPDA-PFMB dimer and the torsion angles defining the backbone conformation are shown in *Figure 3*. Molecular modelling showed that the monomer repeat of homopoly(BPDA-PFMB) can vary between 19.80 and 20.40 Å, depending on the biphenyl and imide–phenyl torsion angles. The minimum energy conformation has a repeat of 20.30 Å, in good agreement with the observed data.

Incorporation of 30% PMDA-PFMB results in a dramatic change in the X-ray pattern, in that the equatorial and off-meridional reflections become much more diffuse, indicating a reduction in lateral order. The observed layer line *d*-spacings for all three preparations of 70/30 copoly(BFPF) are given in *Table 2*. The layer lines are periodic and have almost the same *d*-spacing as those for homopoly(BPDA-PFMB). The discrepancies for layer lines 6 and 7 may be due to arcing of off-meridional intensity. This suggests that 70/30 copoly(BFPF) contains homopolymer blocks of the major component. There is no evidence for the non-periodic diffraction effects expected for a random copolymer. Diffractometer scans of the intensive third layer line reflection for homopoly(BPDA-PFMB) and 70/30 copoly(BFPF) along the fibre axis direction are shown in *Figure 4*. Although there is a change in peak width, it can be seen that the peak position does not shift with introduction of the PMDA comonomer. The *d*-spacings for the layer line predicted for the random copolymer are listed in *Table 2*, and can be seen to differ from the observed layer line *d*-spacings beyond the range of experimental error.

Preparations II and III were the result of efforts to generate more random monomer sequences in 70/30 copoly(BFPF). However, their fibre diagrams were very similar to that for preparation I (*Table 2*). Thus it can be concluded that the reactivity of BPDA and PMDA are very different, since all three specimens of copoly(BFPF) are highly blocky. There is no evidence for the existence of crystalline homopoly(PMDA-PFMB) blocks, but the

Table 1 Comparison of the observed and calculated layer line *d*-spacings for homopoly(BPDA-PFMB)

Layer line	*d* observed (Å)	*d* calculated (Å)
1	20.20 ± 0.2	20.24
2	10.15 ± 0.1	10.12
3	6.748 ± 0.005	6.748
4	5.06 ± 0.03	5.06
5	4.03 ± 0.03	4.05
6	3.36 ± 0.02	3.37
7	2.86 ± 0.03	2.88

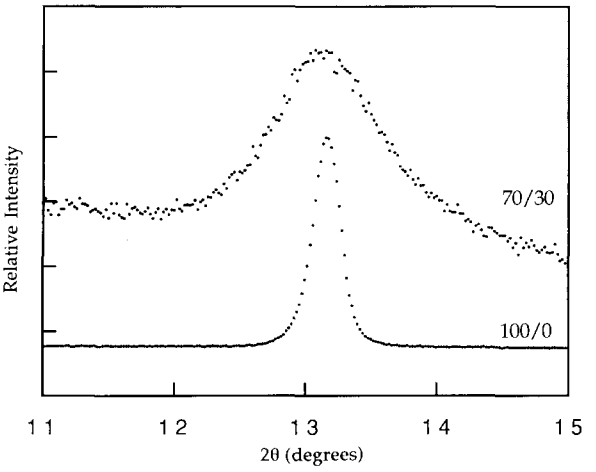

Figure 4 X-ray diffractometer scans along the chain axis direction for the third layer line for homopoly(BPDA-PFMB) and 70/30 copoly(BFPF) (preparation I)

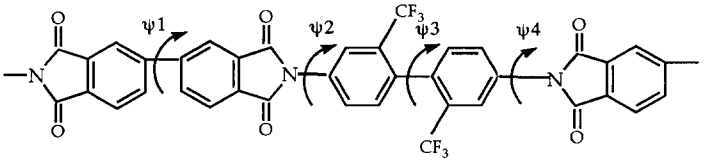

Figure 3 Torsion angles defining the backbone conformation of homopoly(BPDA-PFMB)

Table 2 Observed layer line *d*-spacings for three preparations of 70/30 copoly(BFPF) compared to those predicted for homopolymer and random copolymer structure. The limits of experimental error are the same for all specimens

	d observed (Å)			*d* calculated (Å)	
Layer line	Prep. I	Prep. II	Prep. III	Homopolymer	Random copolymer
3	6.76 ± 0.02	6.70	6.68	6.75	6.82
4	5.08 ± 0.04	5.08	5.09	5.06	5.16
6	3.30 ± 0.03	3.30	3.30	3.37	3.37
7	2.81 ± 0.03	2.82	2.83	2.88	2.87
9	2.24 ± 0.02	2.25	2.25	2.25	2.27
10	2.01 ± 0.02	2.02	2.01	2.01	2.04

Table 3 Crystallite size, paracrystalline distortion parameter g and azimuthal half-width determined for homopoly(BPDA-PFMB) and 70/30 Copoly(BFPF)

	Crystallite size (Å)	Paracrystalline distortion g (%)	Azimuthal half-width (degrees)
Homopoly(BPDA-PFMB)	390±10	1.7±0.1	3.7±0.1
70/30 Copoly(BFPF)	115±5	2.2±0.1	24.4±0.4

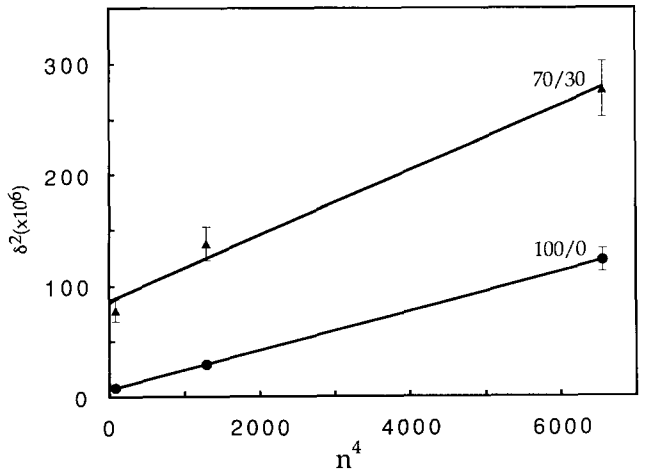

Figure 5 Plot of δ^2 against n^4 for homopoly(BPDA-PFMB) and 70/30 copoly(BFPF); δ is the line width in radians along the chain axis direction for reflection on the nth layer line

introduction of the minor component leads to a decrease in the size of the homopoly(BPDA-PFMB) crystallites. *Figure 5* shows plots of integral half-width δ^2 against order n^4 for the third, sixth and ninth orders of meridional reflections for homopoly(BPDA-PFMB) and 70/30 copoly(BFPF) (preparation I). The crystallite sizes and paracrystalline distortion parameters derived from the $n=0$ intercepts and the slopes of these plots are given in *Table 3*. Introduction of 30% PMDA-PFMB comonomer has more than halved the longitudinal dimensions of the crystallites, which are also much more distorted. Introduction of the comonomer also reduces the drawability of the fibres[18]. Homopoly(BPDA-PFMB) can be drawn up to 10×, whereas the 70/30 copoly(BFPF) can only be drawn 5×. This is correlated with the degree of orientation of the crystallites, as determined from the azimuthal half-widths of the meridional reflections (*Table 3*).

Copoly(BTBD)

Figure 6 shows the X-ray diffraction patterns of the drawn fibre of the homopoly(BPDA-OTOL) and 80/20 copoly(BTBD). For homopoly(BPDA-OTOL), the X-ray data contain sharp Bragg reflections on the equator and 12 layer lines. The d-spacings of the observed layer line are listed in *Table 4*, from which we derive the chain repeat of $c=20.44$ Å. This repeat is slightly larger than that for homopoly(BPDA-PFMB), probably due to a change in the phenyl–phenyl torsion angle necessitated by the presence of trifluoromethyl groups in PFMB. The chemical structure of the BPDA-OTOL dimer and the torsion angles defining the backbone conformation are shown in *Figure 7*. Molecular modelling indicates that the monomer repeat for allowed conformations of BPDA-OTOL can vary between 20.2 and 20.6 Å, and the minimum energy conformation has a repeat of 20.40 Å.

For copoly(BTBD), the X-ray fibre diagrams change progressively with increasing BPDA-PPD content: the equatorial and off-meridional Bragg reflections become more diffuse and gradually disappear, pointing to distortions in a–b plane, as well as possible shifts of the chains with respect to each other along the fibre axis. The observed d-spacings for the laver lines for four

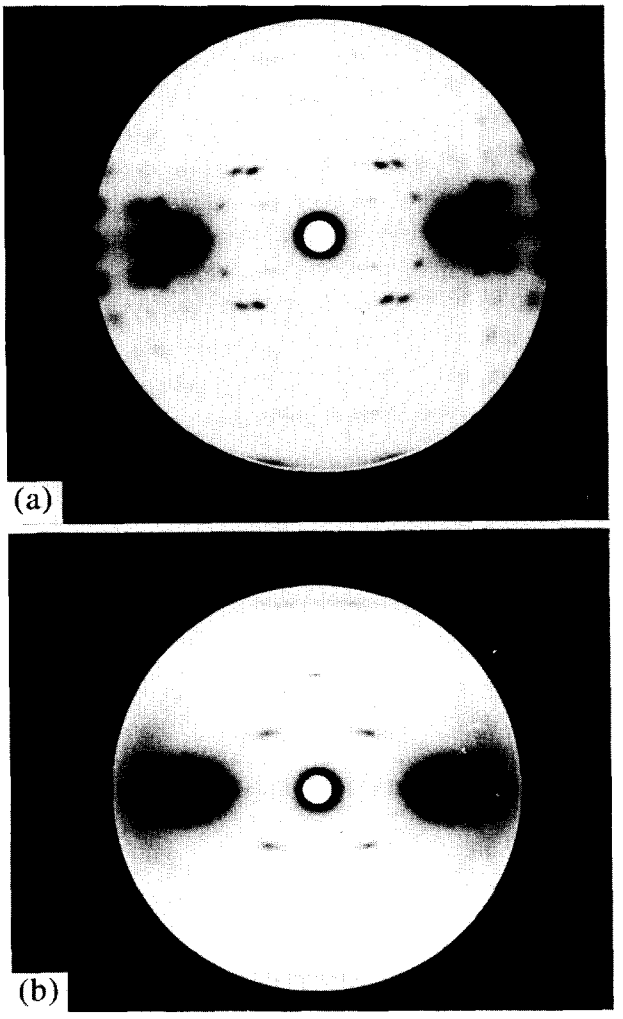

Figure 6 X-ray fibre diagrams of (a) homopoly(BPDA-OTOL) and (b) 80/20 copoly(BTBD)

Table 4 Observed and calculated layer line d-spacings for homopoly(BPDA-OTOL)

Layer line	Observed d-spacing (Å)	Calculated d-spacing (Å)
1	20.40±0.20	20.44
2	10.20±0.15	10.22
3	6.80±0.05	6.81
4	5.108±0.005	5.108
5	4.09±0.03	4.09
6	3.41±0.02	3.40
7	2.93±0.02	2.92
8	2.55±0.02	2.55
9	2.26±0.02	2.27
10	2.03±0.01	2.04

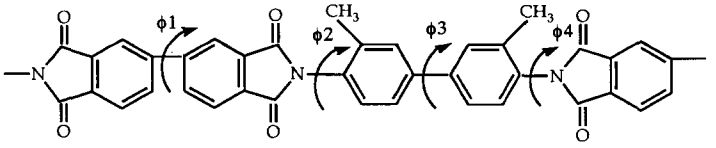

Figure 7 Torsion angles defining the backbone conformation of homopoly(BPDA-OTOL)

Table 5 Observed layer line *d*-spacings of copoly(BTBD) compared to those predicted for homopoly(BPDA-OTOL) and for random copolymer structures

Layer line	BT/BD	*d* observed (Å)	*d* calculated (Å)	
			Homopolymer	Random copolymer
2	80/20	10.12±0.15	10.22	10.15
3		6.81±0.20	6.81	6.89
4		5.123±0.005	5.108	5.136
5		4.05±0.03	4.09	4.07
6		3.38±0.02	3.40	3.39
7		2.90±0.02	2.92	2.92
2	70/30	10.10	10.22	10.10
3		6.74	6.81	6.96
4		5.149	5.108	5.150
5		4.06	4.09	4.04
6		3.37	3.40	3.36
7		2.91	2.92	2.93
2	60/40	9.95	10.22	10.02
3		6.75	6.81	7.16
4		5.161	5.108	5.166
5		4.05	4.09	4.04
6		3.37	3.40	3.32
7		2.91	2.92	2.92
8		2.57	2.55	2.59
2	50/50	9.50	10.22	9.80
4		5.175	5.108	5.182
5		3.99	4.09	4.03
6		3.29	3.40	3.28
7		2.94	2.92	2.92
8		2.57	2.55	2.59

comonomer ratios are listed in *Table 5*. These data are seen to change with monomer ratio, and are suggestive of a random sequence. The *d*-spacings of the meridional maxima predicted for random sequences of the four copolymers are listed in *Table 5*, which are in good agreement with those observed. Diffractometer scans along the fibre axis direction through the intense maximum on the fourth layer line for the homopolymer and four copolymer ratios are presented in *Figure 8a*, where it is seen that the peak shifts to smaller angles with increasing BPDA-PPD content. The profiles predicted for infinite chains of random sequence are shown in *Figure 8b*. The positional agreement is very good; the profiles are narrower than those observed because the calculations are for infinite linear chains, so that for example, we obtain a δ-function for the homopolymer. The profiles can be broadened by considering finite chain length or allowing for slight non-linearity in the chain conformation.

It is striking that the observed line width for the homopolymer is greater than the widths for the copolymers, and that the latter decrease progressively with increasing comonomer content up to 40% BPDA-PPD. (The data for the 50/50 copolymer are not directly comparable because of the different specimen preparation.) This observation is the opposite of that described above for the copoly(BFPF), where introduction of the comonomer leads to increased line width, i.e. reduction of the longitudinal crystallite size as a result of distortions. For copoly(BTBD), it appears that the correlation length along the chain axis, which is a measure of the perfection of the extended conformation, increases with increasing content of minor component. If we use the line widths to determine an apparent longitudinal crystallite size by application of the Scherrer equation, this parameter increases from 190 to 440 Å as the BPDA-PPD content goes from 0 to 40% (*Figure 9*). In fact the difference between the homopolymer and copolymers is even greater than suggested by these apparent widths. The predicted maxima for the random

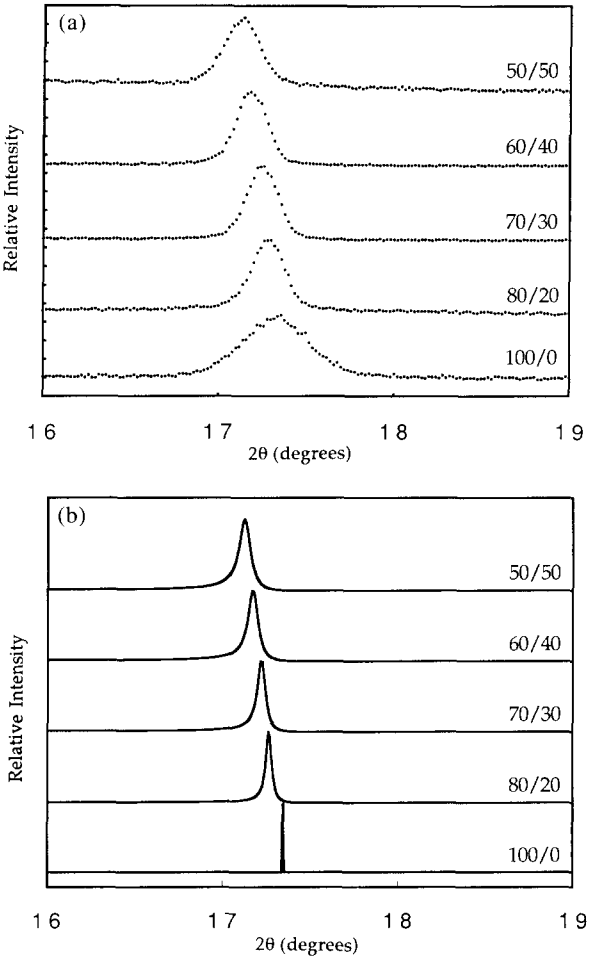

Figure 8 (a) X-ray diffractometer scans along the chain axis direction for the fourth layer line for homopoly(BPDA-OTOL) and 80/20, 70/30, 60/40 and 50/50 copoly(BTBD). (b) Calculated meridional intensity profile on the fourth layer line along the chain axis direction predicted for an infinite chain of random comonomer sequence for 80/20, 70/30, 60/40 and 50/50 copoly(BTBD). The lowest curve shows the position of the predicted maximum for homopoly(BPDA-OTOL)

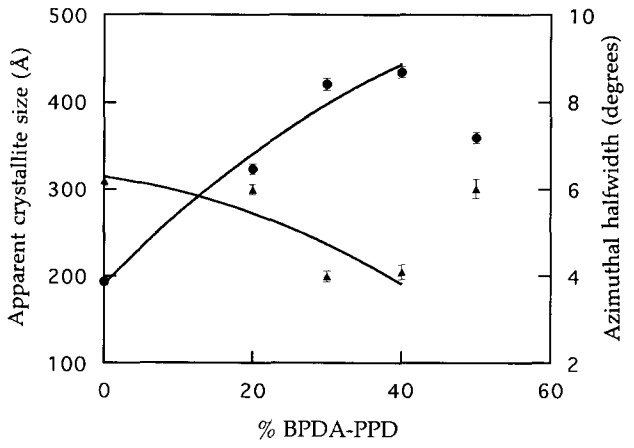

Figure 9 Apparent crystallite size and azimuthal half-width for copoly(BTBD) fibres derived from the fourth layer line meridional reflection, plotted as functions of composition

copolymers have finite width even for infinite linear chains, so that only part of the observed broadening is due to non-linearity. Further analysis of the extent of the distortion in these random copolymer structures is now in progress[21].

Increase in the BPDA-PPD content is also accompanied by an improvement in the drawability[23] and an increase in the degree of orientation (*Figure 9*). These changes parallel the increase in the correlation length for the extended chain conformation, and again contrast with the results for copoly(BFPF), where the presence of 30% PMDA-PFMB reduces the drawability and degree of orientation, and decreases the longitudinal crystallite size.

The above differences probably reflect the different flexibilities of the major and minor components of the two families of copolymers. During spinning, the polymer chains become aligned parallel to the direction of draw, but conformational defects may preclude perfect alignment of chains, and thereby limit the draw ratio. Addition of more flexible monomers may facilitate rearrangement to give a more linear conformation, thereby 'healing' the effect of chemical defects. However, increase in the content of a more rigid component is likely to lead to decreases in drawability, degree of orientation and longitudinal correlation length. Thus it is useful to analyse the conformational freedom of the BFPF and BTBD copolyimides by theoretical modelling.

Molecular modelling

Torsional energy profiles of the rotatable bonds in the BPDA-OTOL, BPDA-PPD, BPDA-PFMB and PMDA-PFMB dimers were calculated using the SYBYL® molecular mechanics software. The results for homopoly(BPDA-OTOL) and homopoly(BPDA-PFMB) are presented in *Figure 10* (0° for each torsion angle corresponds to the planar conformation as shown in *Figures 3* and *7*). In each case the dimer units contain four rotatable bonds. The rotational energy profiles for torsion angles $\phi 1$ and $\phi 3$ in BPDA-OTOL and $\psi 1$ in BPDA-PFMB are essentially the same. The energy barriers for complete rotation about these bonds are $\sim 40\,\text{kcal mol}^{-1}$. For the other two rotatable bonds ($\psi 2$ and $\psi 4$) in BPDA-PFMB, the energy barrier is lower at $25\,\text{kcal mol}^{-1}$. The energy barrier for torsional rotation within the biphenyl is higher than within the imide–phenyl unit. In addition, BPDA-PFMB has three rotatable bonds, compared to only two for BPDA-OTOL. The steric hindrance of the methylene substituent and imide ring inhibits variation of $\phi 2$ and $\phi 4$ in BPDA-OTOL, so that essentially only oscillations in a range of ($\phi 2$ or $\phi 4 \approx$) 60–120° are possible. A similar situation occurs for $\psi 3$ in BPDA-PFMB.

Thus the existence of a larger number of rotatable bonds, and lower energy barriers for complete rotation, lead to higher flexibility for homopoly(BPDA-PFMB) than for homopoly(BPDA-OTOL). Variation of the torsion angle in BPDA ($\phi 1$ or $\psi 1$) has a much greater influence on the conformation than changing the torsions in PFMB and OTOL: a 180° change in $\phi 1$ or $\psi 1$ results in a large change in the direction of propagation of the chain (*Figure 11a*). In order to restore the extended chain conformation, it would be necessary either to change this angle at the next BPDA by 180° (*Figure 11b* (i)) or to change the torsion angles of the other rotatable bonds in the monomer (*Figure 11b* (ii)). Rotations of 180° at two consecutive BPDA units lead to a zig-zag kink defect, which is larger in homopoly(BPDA-OTOL) than in homopoly(BPDA-PFMB). It should also be noted that the chain conformation is more affected by changes in $\psi 2$ and $\psi 4$ in BPDA-PFMB than by changes in $\phi 3$ in BPDA-OTOL. These differences probably explain the fact that homopoly(BPDA-PFMB) has better drawability and higher longitudinal crystallite size than are observed for homopoly(BPDA-OTOL).

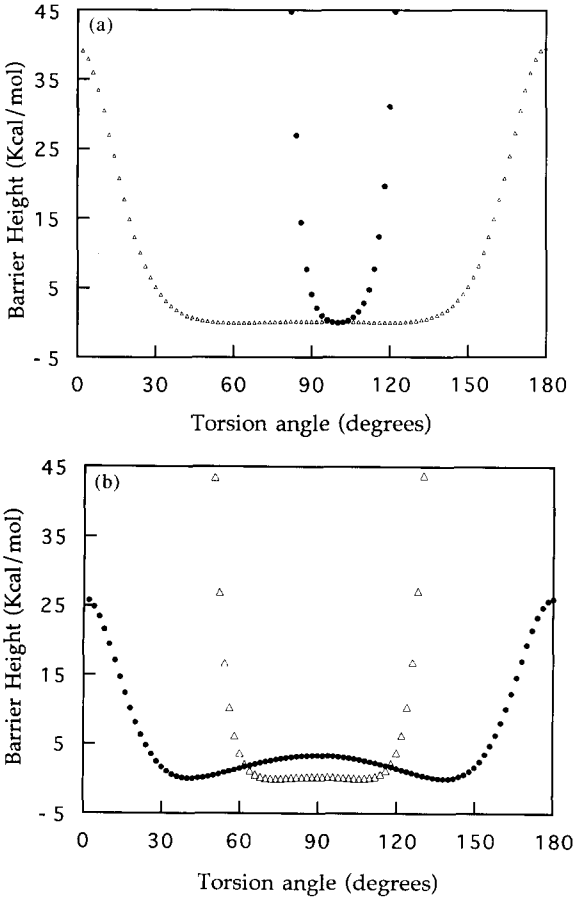

Figure 10 (a) Calculated energies for torsion angles $\psi 1$ (△) and $\psi 3$ (●) in BPDA-PFMB and $\phi 1$ and $\phi 3$ (△) in BPDA-OTOL. (b) Calculated energies for torsion angles $\psi 2$ and $\psi 4$ (●) in BPDA-PFMB and $\phi 2$ and $\phi 4$ (△) in BPDA-OTOL

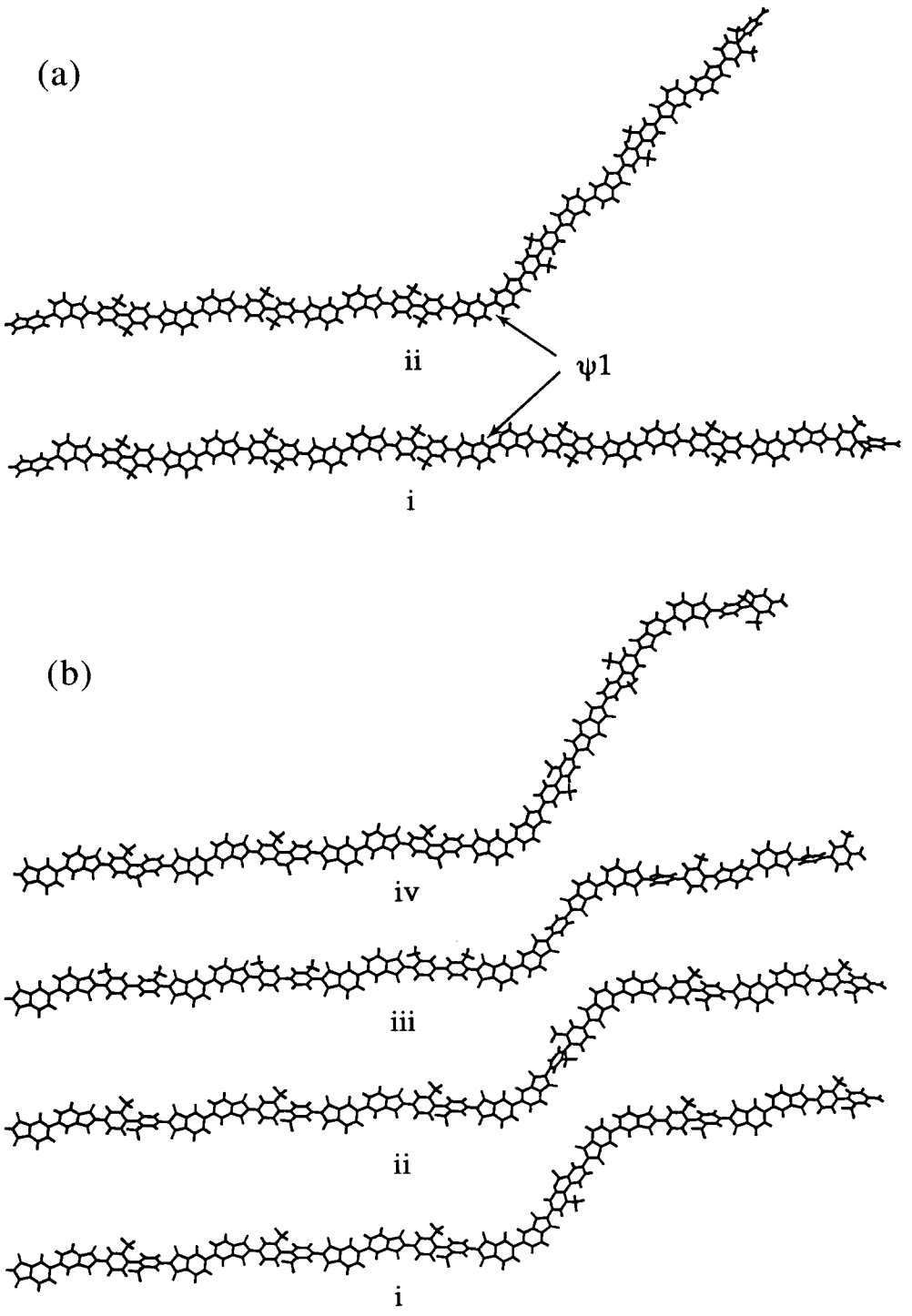

Figure 11 (a) Models of the conformation of homopoly(BPDA-PFMB): (i) extended chain; (ii) kink-defect chain due to rotations of 180° at $\psi 1$. (b) Zig-zag kink defects in copoly(BFPF) and copoly(BTBD): (i) two consecutive 180° rotations at $\psi 1$ in BPDA-PFMB; (ii) rotation of 180° at $\psi 1$ followed by changes of the torsion angles at $\psi 1$ and $\psi 3$ in BPDA-PFMB; (iii) shorter zig-zag kink at a PPD unit in copoly(BTBD); (iv) longer zig-zag kink at a PMDA unit in copoly(BFPF)

Introduction of BPDA-PPD units into homopoly-(BPDA-OTOL) corresponds to addition of more flexible units to the chains, because rotation around imide–phenyl and phenyl–imide bonds of BPDA-PPD ($\phi 6$ and $\phi 7$) is not as restricted as is the case in the imide–phenyl of BPDA-OTOL. The rotational energy barrier at $\phi 3$ in BPDA-OTOL is $\sim 40\,\text{kcal mol}^{-1}$ while for $\phi 6$ and $\phi 7$ the barriers are only $\sim 25\,\text{kcal mol}^{-1}$, the same as for $\psi 2$ in BPDA-PFMB. Therefore, the possible defects due to changes in $\phi 1$ in BPDA-OTOL may be compensated by change in the torsion angles in BPDA-PPD (see (iii) in *Figure 11b*). In contrast, introduction of PMDA-PFMB units into homopoly(BPDA-PFMB) decreases the chain flexibility, since PMDA-PFMB has one less rotatable bond (see (iv) in *Figure 11b*). This could lead to an increase in the content of conformational defects and consequently

to a decrease of drawability and a reduction of longitudinal crystallite size. The presence of a more rigid coplanar structure is confirmed by the shift of glass transition to higher temperature with the increasing content of PMDA-PFMB[18], and observation of a lower Kuhn segment length, which is characteristic of a more flexible chain[24].

CONCLUSIONS

The X-ray data show that homopoly(BPDA-PFMB) and homopoly(BPDA-OTOL) fibres have highly ordered crystalline structures. Molecular modelling of isolated chains predicts fibre repeats that are close to those observed. X-ray data for the 70/30 copoly(BFPF) indicate a highly blocky copolymer and the presence of crystalline $(BPDA\text{-}PFMB)_n$ blocks. Introduction of the 30% more rigid PMDA-PFMB monomer reduces the crystallite size from 390 to 115 Å, which correlates with a deterioration of drawability and degree of orientation and an increase in paracrystalline distortion. In contrast, the data for four compositions of copoly(BTBD) point to random comonomer sequences. Introduction of the more flexible BPDA-PPD monomer is accompanied by an increase in the correlation length for the extended chain conformation, an improvement of the drawability, and an increase in the degree of orientation.

ACKNOWLEDGEMENTS

This work has been supported by National Science Foundation (NSF) Grant No. EEC 91-08700, the State of Ohio Department of Development, and the Edison Polymer Innovation Corporation (EPIC) through the Center for Molecular and Microstructure of Composite (CMMC) at Case Western Reserve University and the University of Akron.

REFERENCES

1 Mittal, K. L. (Ed.) 'Polyimides: Synthesis, Characterization and Application', Plenum Press, New York, 1984
2 Yang, H. H. 'Aromatic High-Strength Fibers', Wiley, New York, 1989
3 Bessonov, M. I., Koton, M. M., Kudryavtsev, V. V. and Laius, L. A. 'Polyimides: Thermally Stable Polymer', Consultants Bureau, New York, 1983
4 Du Pre, D. B. in 'Encyclopedia of Chemical Technology' (Eds R. E. Kirk, D. F. Othmer, H. F. Mark, M. S. Grayson and D. Eckrath), Wiley Interscience, New York, 1977
5 McFarlane, F. E., Nicely, V. A. and Davis, T. G. in 'Contemporary Topics in Polymer Science' (Eds E. M. Pearce and J. R. Schaefgen), Plenum Press, New York, 1977, Vol. 2, pp. 109–138
6 *Plastics World* 1984, **42**, 8
7 Krause, S., Haddock, T. B., Price, G. E. and Adams, W. W. *Polymer* 1988, **20**, 195
8 Koshi, M., Uruji, T., Jizaka, T., Mita, J. and Jokota, R. *J. Polym. Sci., Polym. Lett. Edn* 1987, **25**, 441
9 Shen, D., Wu, Z., Liu, J., Wang, L., Lee, S., Harris, F. W., Cheng, S. Z. D., Blackwell, J., Wu, T. M. and Chvalun, S. *Polym. Polym. Compos.* 1994, **2**, 149
10 Gutierrez, G. A., Chivers, R. A., Blackwell, J., Stamatoff, J. B. and Yoon, H. *Polymer* 1983, **24**, 937
11 Blackwell, J., Gutierrez, G. A. and Chivers, R. A. *Macromolecules* 1984, **17**, 1219
12 Biswas, A. and Blackwell, J. *Macromolecules* 1987, **20**, 2997
13 Blackwell, J., Cageao, R. A. and Biswas, A. *Macromolecules* 1987, **20**, 667
14 Mitchell, G. R. and Windle, A. H. *Colloid. Polym. Sci.* 1985, **263**, 230
15 Harris, F. W. and Hsu, S. L. C. *High Perform. Polym.* 1989, **1**, 1
16 Harris, F. W. in 'Polyimide' (Eds D. W. Wilson, H. D. Stenzenberger and P. M. Hergenrother), Chapman and Hall, New York, 1990, Ch. 1
17 Cheng, S. Z. D., Wu, Z., Eashoo, M., Hsu, S. L. C. and Harris, F. W. *Polymer* 1991, **32**, 1803
18 Arnold, F. E. Jr, Shen, D., Lee, C. J., Harris, F. W., Cheng, S. Z. D. and Starkweather, H. W. Jr *J. Mater. Chem.* 1993, **3**, 183
19 Harris, F. W. and Cheng, S. Z. D. Unpublished data, 1993
20 Hosemann, R. and Wilke, W. *Macromol. Chem.* 1968, **118**, 230
21 Wu, T. M., Chvalun, S. N. and Blackwell, J. In preparation
22 Takahashi, N., Yoon, D. Y. and Parris, W. *Macromolecules* 1984, **17**, 2583
23 Wu, T. M., Chvalun, S. N., Blackwell, J., Cheng, S. Z. D., Wu, Z. and Harris, F. W. *Acta Polym.* in press
24 Miwa, T., Tawata, R. and Numata, S. *Polymer* 1993, **34**, 621